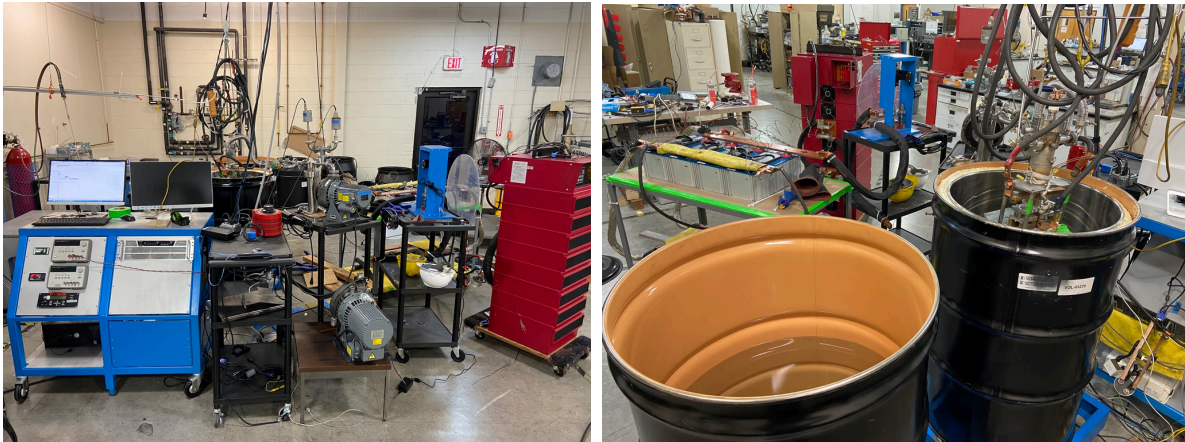


SunCell® Water bath calorimeter:

Water bath calorimetry (WBC) can be a highly accurate method of energy measurement due to its inherent ability for complete capture and precise qualification of the released energy. However, submersion of the SunCell® in a water bath lowers its wall temperature significantly relative to operation in air. The hydriño reaction rate increases with temperature, current density, and wall temperature wherein the latter facilitates a high molecular hydriño permeation rate through the wall to avoid product inhibition. In order to evaluate the absolute output energy produced by Brilliant Light Power’s SunCell® while maintaining favorable operating conditions of high gallium and wall temperatures, the cell was operated suspended on a cable for the duration of a power production phase and then the cell was lowered into a water bath using an electric winch. The thermal inventory of the entire submerged cell assembly was transferred to the water bath (Figures 1A-D) in the form of an increase in the water temperature and steam production. Following equilibration of the cell temperature to that of the water bath, the cell was hoisted from the water bath and the increase in thermal inventory of the water bath was quantified by recording the bath temperature rise and the water lost to steam by measuring the water weight loss.

Figures 1A-D. SunCell® Water Bath Calorimeter Schematics.



(A)

(B)



(C)

(D)

These WBC tests featured cylindrical cells, each incorporating an internal mass of liquid gallium which served as a molten metal reservoir with a corresponding thermal sink. The molten gallium also acted as an electrode in the formation and operation of the very-low voltage, high-current hydrino-reaction-driven plasma while a tungsten electrode acted as the opposing electrode when electrical contact was made between the electrodes by electromagnetic pump injection of the molten metal from the reservoir to the W electrode. The plasma formation depended on the injection of hydrogen gas with about 8% oxygen gas and the application of high current at low voltage using a DC power source.

Specifically, SunCells® engineered to maintain the hydrino reaction shown in Figures 1A-C each comprised (i) a reactor cell, (ii) a reaction cell chamber, (iii) a molten metal injector system with an electromagnetic pump driven by a DC power supply and a gallium reservoir that served as an electrode, (iv) a counter electrode, (v) gas flow systems, (vi) bus bars to the electrodes, (vii) an ignition power source, and (viii) voltage, current, and temperature sensors. The reactor cell was a Type 347 stainless steel (SS) cylindrical tube measuring 7.3 cm ID, 19.7 cm in height, and 0.635 cm thick with 3.17 mm thick boron nitride (99%) liner to provide an electrical insulation barrier and a physical barrier to prevent the internal gallium inventory from alloying with the stainless steel at temperatures above 500 °C. The cell was pressure leak checked at the shop following fabrication, and the high-vacuum integrity of the cell and gas and vacuum connections was confirmed by mass spectroscopy using a residual gas analyzer (Ametek Dycor Q100M). The cylindrical reaction cell chamber of about 50 ml plasma volume was between the electrodes and confined internal to the BN liner. The molten metal injection system comprised 0.9 kg of molten gallium in the bottom of the reactor that served as a reservoir of gallium and an electrode, a Type 304 SS injection tube with a W injector nozzle submerged in the gallium by 0.7 cm, and a DC electromagnetic pump. An electrical bus bar (W solid rod, 1 cm OD) penetrated the bottom of the reservoir through a Swagelok fitting (SS-10MO-1-6W) and was submerged in the gallium by at least 2.54 cm such that at least one of the injector nozzle and the molten gallium served as an electrode. The opposing counter electrode oriented along the negative z (vertical) axis (Figure 2) received injected gallium from the injector nozzle to create an electrical connection between the two electrodes. The counter electrode comprised a feed through (solid sealing technology, part # FA10775) in a flange (Kurt Lesker 4.5 inch CF flange) sealed at the top of the reaction cell chamber by a gasket (silver plated Cu), a W bus bar 1.37 cm diameter with male threads on each end to screw-in collect to a 2.54 cm diameter copper bus bar on the internal side of the feed through on the top end and the W electrode on the opposite end. The bus bar was covered by an electrically insulating fused quartz sheath (Technical Glass Products, 2.7 cm ID x 5.1 cm long) sealed with an inner quartz collar that penetrated into the feed through and was further sealed with an alumina-based cement (Resbond 989) at the feed-through end. The counter electrode, a concave refractory metal electrode (W 3.8 cm OD, 1.37 cm height, with a concavity of 2 cm at the apex), screwed onto a threaded end of the W bus bar and pressed the quartz sheath against the top flange at the opposite end of the sheath. Reactants comprising nascent H₂O catalyst and a source of atomic hydrogen was provided by separately controlled H₂ (Praxair UHP, 99.999%) and 8% O₂ (Praxair industrial grade) flows using two mass flow controllers (MKS Model PR4000-F2V1N with MKS Model #1179A53CR1BVS for 2500 SCCM of H₂ flow and MKS Model #M100B12R1BB for 200 SCCM of O₂ flow) that were each calibrated with a rotameter (Dwyer Instruments VA10423, accurate to +/- 2%). The gases were mixed in an oxyhydrogen torch and flowed through a recombiner chamber comprising 1 g of a granular platinum catalyst (10% Pt/Al₂O₃ beads from Alfa Aesar) heated to greater than 90 °C by the H₂+1/2O₂ recombination reaction before flowing into the reaction cell chamber using Swagelok fittings (SS-400-6-4W). The ignition system comprised either a switch-mode rectifier or a capacitor bank that supplied high-current DC electrical power sufficient to cause the reactants to react to form plasma. The current was measured with a Hall sensor and the voltage was measured with a PicoScope. The temperature of the molten gallium reservoir was measured using 2 K-Type ungrounded thermocouples rated to

1335 °C. The thermocouples penetrated the side section of the reaction cell chamber through Swagelok fittings (SS-200-6-2W) extended about 1 cm into the gallium.

Figures 2A-C. SunCell® Schematics.

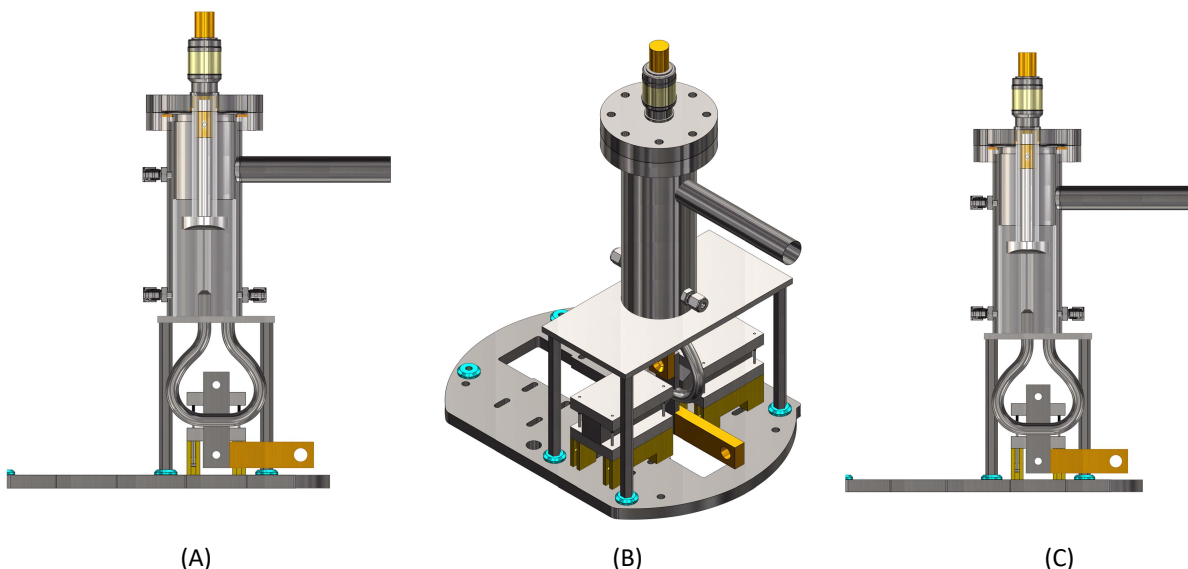
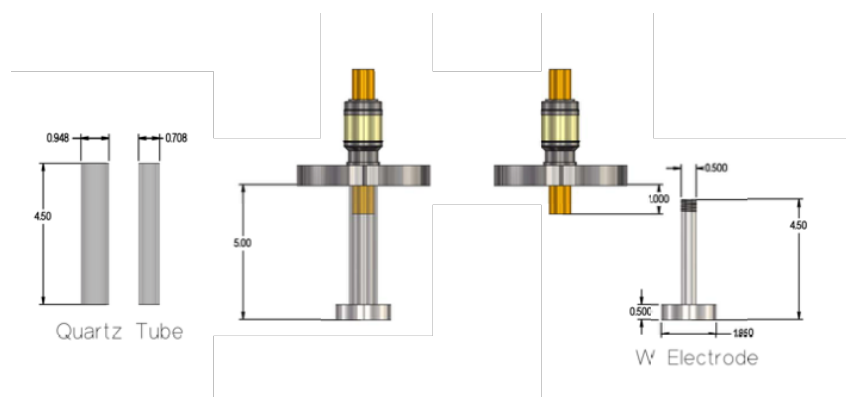


Figure 3. SunCell® Electrode Assembly Schematics.



Prior to the start of the reaction, the cell was connected to a scroll vacuum pump (Anest Iwata Model ISP-250) by a 2.54 cm OD stainless steel vacuum line with an intervening liquid nitrogen cryotrap. All unwanted gases were removed down to a pressure of approximately 40 mTorr (MKS Model #626A11TBE 10 Torr gauge and MKS Model #626A13TEE 1000 Torr gauge). During operation with flowing gas reactants, the pressure was maintained under 5 Torr. Prior to operation, the pressure gauges were verified for accuracy within +/- 1% using the same unit that was vendor calibrated.

The reaction within the cell was maintained using two separate electrical systems: an electromagnetic (EM) pump system to complete the circuit between the two electrodes within the cell, and an ignition system to supply electrical input energy to initiate the reaction. The EM pump was powered by a programmable DC power supply (Model: Matsusada Precision REK10-1200) set to current control mode wherein the current output directly controlled the flow rate of liquid Ga through the pump tube assembly. During typical operation, the Ga flow rate

was measured to be approximately 40 cm³/sec wherein the voltage and current across the EM pump was about 0.1 V and 200 A, respectively. The ignition circuit was powered by a LabVIEW-controlled (National Instruments) switch-mode rectifier (Model: American CRS Q500 IP32) rated to a maximum of 50V/1500A. The negative and positive terminals of the rectifier were connected to a solid tungsten (W) rod anode and a liquid Ga cathode, respectively. Alternatively, the polarity was reversed. The excess power was observed to be strongly dependent on the applied current. So, tests were also performed using an initial and peak current in the range of 3000-6000 A that was supplied by a capacitor bank charged to 48 V by the switch-mode rectifier. The capacitor bank comprised either four or eight Maxwell Technologies modules (Model #BMOD0165 P048 C01) connected in parallel. Each module was rated to 48 V with a capacitance of 165 F wherein four or eight modules in parallel increased the capacitance to 660 F or 1320 F, respectively. For the ignition circuit, the electrical response was recorded on a high sampling rate and high-resolution oscilloscope (Model: PicoScope 5000 Series) using a voltage differential probe (Model: PicoTech TA041, ±70V) and a DC Hall effect sensor (Model: GMW CPCO-4000-77-BP10, ±4 kA). The Hall sensor was redundantly calibrated with three Matsusada DC power supplies (Model: Matsusada Precision REK10-1200) that were current calibrated by the manufacturer. The voltage probe was calibrated using a standardized voltage source (Model: Agilent E3631A +/- 0.01 V).

The ignition power was terminated after a predetermined power run duration wherein the gallium temperature reached an upper temperature limit, beyond which thermally induced failure of the reactor could occur. Following ignition power shut off, all vacuum and gas connections were disconnected, and the SunCell® was sealed and completely submerged into a calorimeter water bath. The primary enclosure for the water bath comprised of a stainless steel cylindrical tank (22" diam. x 36" tall) inserted inside a larger steel tank (27.5" diam. x 44" tall) where the space in between the tanks was filled with polyurethane insulation to prevent thermal losses to the surrounding environment. The calorimeter water tank also contained two water circulators (Franklin Electronics Little Giant 5-MSP 125 W and Shysky Tech Speed Adjustable DC 24V 50A-2450A Small Water Pump Micro Solar Circulation Submersible Pump 3600L/H 5M) each fitted with a plastic manifold to create water jets directed at the cell walls to provide cooling by forced convection and tank mixing to prevent the formation of any heat gradients within the water bath for increased accuracy in the calorimetric measurements. Each circulator was first primed by operating in a third water tank, transferred to the calorimeter tank, operated to perform the mixing, and removed following the recording of the bath temperature so that the weight of the water loss could be determined. The temperature of the water bath was measured using two high-accuracy digital thermistors (Model: Parr 6775A Digital Thermometer) with a resolution of +/-0.001 °C.

For all experiments, the tank was filled with 126 kg of deionized (DI) water measured with a flow meter (Carlson Model #062JLP, accurate to 0.01 gal +/- 1.5%). The accuracy of the flow meter was verified by independently measuring the weight of the water on a digital scale with an accuracy of ± 0.1 kg. This entire quantity of water was first heated to above 32 °C to prevent the solidification of the liquid Ga within the cell when submerged. The electrical conductivity of the water was carefully monitored between every experiment using a handheld water conductivity meter (Model: Ohaus ST20C-B) to monitor the potential for external cell corrosion when in contact with elevated-temperature, aerated water. A conductivity value under 15 µS/cm was deemed as acceptable, with the DI water being replaced if the threshold was exceeded.

At the time of initial immersion, the wall temperature of the reactor was very hot, (e.g. 300-700 °C) which gave rise to immediate flash boiling on the cell wall-water interface. The boiling created a significant amount of steam bubbles that floated to the surface of the water bath and escaped. Therefore, the calorimetric measurement of power balance measured by the water bath comprised two separate components, (i) heat inventory of the water due to heating determined from the water mass, heat capacity, and the change in temperature during the experiment, and (ii) heat of vaporization due to water boil off determined by the heat of water vaporization and

mass loss to steam. These calorimetric results depend critically on the accurate measurement of the water loss from the bath by vaporization during a test. A lever balance system was used to measure the water loss by weight loss to better than 1% accuracy.

Specifically, the water weight loss (+/- 0.5 g) was determined using a mechanical balance comprising a 1st class lever wherein a steel frame measuring 66" long x 28" wide was mounted on a cylindrical shaft with 2 rolling bearings, which functioned as a fulcrum. The calorimeter tank with the water jet was placed on one side of the lever, while an identical tank filled with about 200 kg of water was placed on the other side as a counterweight. The two tanks were welded in place on the frame such that the moments on either side of the fulcrum were balanced.

To perform a gravimetric measurement of water loss in the calorimeter, with the cell removed from the calorimeter, water was added to the counterweight tank until the weight in both tanks was perfectly balanced. A digital scale (MyWeigh® i5500) with an accuracy of ± 0.1 g was then placed under the counterweight and the amount of water in the tanks was adjusted such that the counterbalance was slightly heavier than the calorimeter tank and the scale would read a stable, non-zero number. Since the scale balances the torques on the arms of the lever in proportion to the weight differential, the reading on this calorimeter scale was calibrated. Using an Ohaus scale (Model # +/- 0.001g), water was removed from the calorimeter tank in gravimetrically measured aliquots, and the corresponding change in weight on the calorimeter scale was recorded. This data was used to form a calibration curve to minimize the error in the calorimeter scale readings.

After the power run was completed and the cell was lowered into the calorimeter water tank, the cell was left to cool down until the cell and the water bath were at the equilibrium temperature. The final temperature recorded at this stage was then used to calculate the heat capacity energy captured by the calorimeter and that remaining in the cell components. The data from the thermistors was then used to calculate the output energy Q by using the thermal energy equation that is a summation over all heat inventories:

$$Q = \sum_i m_i C_{p_i} \Delta T_i \quad (1)$$

where m_i is the mass of the water and each component within the cell [kg], C_{p_i} is the corresponding specific heat capacity [J/kg·K], and ΔT is the corresponding total change in temperature [K]. The specific heat of each component was taken from the literature [1]. Thus, the total output energy was determined by adding the cumulative energy values of all components within the cell.

Subsequently to thermal equilibration, the cell and water jets were removed from the calorimeter tank and the net change in weight on the scale was recorded. This change in weight was then compared to the calibration curve to find an accurate measurement of water loss (+/- < 1%), which was then used to calculate the enthalpy term due to vaporization. This loss was corrected by a calibration of the water loss due to wetting the cell by separately dipping a dry cell and recording the water loss by weight. The heat of vaporization from the initial temperature at the time of cell submersion to 100 °C was determined from experimental data in the literature [2] wherein the positive contribution to the energy and power balances due to escaping superheated steam due to the very high cell temperature was ignored.

An additional factor in the total energy balance that required consideration was the thermal contribution from the water circulator and the ambient-temperature evaporative water loss in absence of heat addition in the tank over the entire duration of the heat transfer from the cell to the water, T_t . In typical operation, the water circulator was running from the point of cell submersion until the cell temperature and water bath temperature had reached equilibrium. A calibration experiment was performed in which the circulator alone was run for the known duration T_t in a water bath with an identical setup to that in the experiments to determine its heat input into the

water bath and the heat corresponding to ambient evaporative loss measured by weigh loss. This contribution was then subtracted from the total output energy that was determined by the sum of the heat capacity energy and the enthalpy due to vaporization of the cell, as determined by the methods given *supra*.

To improve the accuracy of the output energy calculations, the thermal losses from the cell wall exterior to the surroundings during the duration of the power run and the time between termination of the ignition power and the cell submersion had to be considered. Therefore, power experiments were conducted where the cell was heated to various temperatures, and the cool down curve over time was modeled to achieve a good fit to the empirical data. This model developed by Dr. M. Nansteel and the time for transfer into the water bath were used to determine the heat loss contribution to the laboratory due to radiation, convection, and conduction [3].

The energy balance of the SunCell® was determined using the input energy and total output energy, and the corresponding average powers were given by each energy divided by the duration of the power run. The calculations for total electrical input energy for a given experiment were performed by first computing the input power using the voltage and current data recorded by the oscilloscope. The resulting data was then subjected to a point-by-point integration to compute the total energy over the duration of the experiment. The calorimetric measurement for total output power was calculated from the sum of four separate components given *supra*: (i) the heat loss from the cell during ignition, shut down, and submersion, (ii) the heat inventory of the water and cell components determined from the corresponding mass, heat capacity, and the change in temperature (Eq. (1)) during the experiment, (iii) the heat of vaporization due to flash boiling determined by the heat of vaporization of water and the total water loss, and (iv) the heat contribution due to stirring the water bath and background evaporation. There was no chemical change observed in cell components as determined by energy dispersive X-ray spectroscopy (EDS) performed on the gallium following the reaction. The power from the combustion of the H₂/ 8% O₂ fuel and HOH catalyst source was limited by the trace oxygen and was negligible. The input power from the EM pump power was also negligible.

1. F. P. Incropera, D.P. DeWitt, *Fundamentals of Heat and Mass Transfer*, Wiley (1996).
2. G. J. Van Wylen, R. E. Sonntag, C. Borgnakke, *Fundamentals of Classical Thermodynamics*, Wiley (1994).
3. https://brilliantlightpower.com/pdf/Nansteel_Molten_Metal_Calorimetry_Data_and_Analysis_Jan_2020.pdf.